



Title	Effects of Al and P Additions on As-cast Austenite Grain Structure in 0.2 mass% Carbon Steel
Author(s)	Kencana, Surya; Ohno, Munekazu; Matsuura, Kiyotaka; Isobe, Kohichi
Citation	ISIJ International, 50(12), 1965-1971 https://doi.org/10.2355/isijinternational.50.1965
Issue Date	2010-12-15
Doc URL	http://hdl.handle.net/2115/75400
Rights	著作権は日本鉄鋼協会にある
Type	article
File Information	ISIJ Int. 50(12)_ 1965-1971 (2010).pdf



[Instructions for use](#)

Effects of Al and P Additions on As-cast Austenite Grain Structure in 0.2 mass% Carbon Steel

Surya KENCANA,¹⁾ Munekazu OHNO,²⁾ Kiyotaka MATSUURA²⁾ and Kohichi ISOBE³⁾

1) Graduate Student, Graduate School of Engineering, Hokkaido University, Kita 13 Nishi 8, Kita-ku, Sapporo, Hokkaido 060-8628 Japan. 2) Division of Materials Science and Engineering, Faculty of Engineering, Hokkaido University, Kita 13 Nishi 8, Kita-ku, Sapporo, Hokkaido 060-8628 Japan. 3) Muroran R&D Laboratory, Nippon Steel Corporation, 12 Nakamachi, Muroran 050-8550 Japan.

(Received on April 15, 2010; accepted on September 1, 2010)

Effects of addition of P and simultaneous additions of Al and P on as-cast γ grain structures of 0.2 mass% C steel have been investigated by means of permanent mold casting. The as-cast γ grain structure consists of Coarse Columnar Grain (CCG), Fine Columnar Grain (FCG) and Coarse Equiaxed Grain (CEG) regions from the mold side to center of the ingot. The single addition of P increases the FCG region in which short axis diameter of the columnar γ grain is comparable to the primary dendrite arm spacing. The simultaneous additions of Al and P also lead to refinement of the structure and, importantly, the complete refinement of the as-cast γ grain structure, *viz.*, the structure without CCG and CEG regions was obtained even with a small amount of P addition when Al was added. The EPMA analysis showed that the refinement is associated with P segregation at interdendritic regions which is enhanced by Al addition. From thermodynamic calculation, it was demonstrated that high P concentrations stabilize δ and liquid phases at lower temperatures and produce the pinning effect on the growth of γ grains at interdendritic regions.

KEY WORDS: carbon steel; solidification; δ - γ transformation; grain refinement; aluminum; phosphorous; segregation; pinning effect.

1. Introduction

The Continuous Casting (CC) process has undergone remarkable technological progresses which have enabled implementation of near-net-shape castings, *i.e.*, thin-slab and strip castings.^{1,2)} Coarsening of as-cast γ -austenite grain structure, however, remains as a major problem in the CC processes of medium carbon steels. In the conventional CC process, the formation of the coarse γ grains causes surface cracks in bending or straightening process.³⁾ In the near-net-shape CC process, also, the formation of the coarse γ grains causes the surface cracks during direct rolling process of the thin-slab⁴⁾ and it results in the coarse final structure of the strip.⁵⁾ Therefore, the refinement of as-cast γ grain structure is one of the most important subjects to resolve these problems.

The studies on evolution of γ grain structure during solidification and sub-sequent cooling in the medium carbon steels revealed that the addition of alloying elements produces profound effects on the γ grain size.^{6,7)} The refinement of as-cast γ grain structure was attempted by lowering the temperature for completion of γ transformation/solidification, T_γ , or by stabilizing fine precipitates of carbide or nitride at high temperatures.^{8–14)} The addition of δ -ferrite stabilizing elements such as Nb, V and Mo extends the δ + γ region in the phase diagram toward lower temperatures, which leads to refinement of as-cast γ grain

structure due to pinning effect of the δ phase on the γ grains.^{15,16)} Moreover, it was reported that P addition led to the refinement of as-cast γ grain structure in 0.1 mass% C steel.^{8–10)} It was discussed that the increase in P concentration significantly lowers T_γ and P segregation developed during casting process provides the pinning effect. In our previous study, we investigated the effects of Al addition on the as-cast γ grain structure in 0.2 mass% C steel.¹⁴⁾ It was observed that the Al addition leads to the refinement of the γ grain structure obtained by permanent mold casting. The γ grain structure consisted of Coarse Columnar Grain (CCG), Fine Columnar Grain (FCG) and Coarse Equiaxed Grain (CEG) regions. The increase of Al concentration resulted in the refinement of γ grain structure due to the increase of the FCG region at the expenses of the other coarse regions. The EPMA analysis and thermodynamic calculation revealed that the AlN phase is not responsible for the refinement, while the addition of Al is considered to enhance P segregation at interdendritic regions which lowers T_γ locally and results in the refinement.

As mentioned above, our recent study demonstrated that Al addition leads to refinement of as-cast γ grain structure and this refinement is considered to stem from enhancement of P segregation at the interdendritic regions. However, the following points remain to be clarified: 1) the effect of single addition of P on the as-cast γ grain structure in 0.2 mass% C steel, 2) the effect of simultaneous addi-

tions of Al and P and 3) the direct evidence for the enhancement of P segregation due to Al addition. The purpose of this study is to clarify these points. First, we investigate the effects of single addition of P. We then investigate the effects of simultaneous additions of Al and P, from which the direct evidence for enhancement of P segregation due to Al addition can be demonstrated.

2. Experimental Procedures

The carbon steel used in the present study is a 0.2 mass% C steel rod. The Al and P concentrations in this base steel are 0.04 and 0.015 mass%, respectively. The Al and P concentrations of our focus ranged from 0.04 to 1.04 mass% and from 0.015 to 0.1 mass%, respectively. The compositions of all the samples used in this study are shown in **Table 1**. The sample weight was about 250 g. It was placed in a cylindrical magnesia crucible with an inner diameter of 30 mm and a depth of 90 mm. The sample was melted at 1550°C inside a SiC electric furnace under an Ar atmosphere. After holding for 1 h, the melt was cast into a steel mold which was held at room temperature. The detailed shape and size of the steel mold can be found in Ref. 11).

Table 1. The chemical compositions of all the samples made in the present study in mass%.

Sample	C	Si	Mn	P	S	Al	N	O
1(base steel)	0.199	0.2	0.8	0.015	0.007	0.04	0.006	0.002
2	0.199	0.2	0.8	0.02	0.007	0.04	0.006	0.002
3	0.199	0.2	0.8	0.035	0.007	0.04	0.006	0.002
4	0.199	0.2	0.8	0.05	0.007	0.04	0.006	0.002
5	0.199	0.2	0.8	0.075	0.007	0.04	0.006	0.002
6	0.199	0.2	0.8	0.1	0.007	0.04	0.006	0.002
7	0.199	0.2	0.8	0.015	0.007	0.1	0.006	0.002
8	0.199	0.2	0.8	0.035	0.007	0.1	0.006	0.002
9	0.199	0.2	0.8	0.015	0.007	0.54	0.006	0.002
10	0.199	0.2	0.8	0.035	0.007	0.54	0.006	0.002
11	0.199	0.2	0.8	0.05	0.007	0.54	0.006	0.002
12	0.199	0.2	0.8	0.075	0.007	0.54	0.006	0.002
13	0.199	0.2	0.8	0.1	0.007	0.54	0.006	0.002
14	0.199	0.2	0.8	0.015	0.007	1.04	0.006	0.002
15	0.199	0.2	0.8	0.035	0.007	1.04	0.006	0.002
16	0.199	0.2	0.8	0.05	0.007	1.04	0.006	0.002

The ingot was then quenched into a strongly stirred iced water bath from a temperature slightly above the Ar_1 transformation temperature. This operation leads to the formation of film-like pro-eutectoid α -ferrite on the γ grain boundary and martensite phase within the γ grain, which enables a clear observation of as-cast γ grain structure. The quenched sample had a rectangular prism shape with a height of 40 mm, a width of 40 mm and a thickness of 20 mm.

The quenched sample was then sectioned transversely at the middle of height. A rectangular area at the center of width on the sectioned plane was selected for microstructural examination with optical microscopes. The rectangular area for the observation extended from the sidewall surface to the center in the thickness direction. The as-cast γ grain and δ dendrite structures were revealed using nital (3 vol%) and Oberhöffer's solutions, respectively. An Electron Probe Micro Analyzer (EPMA) was employed to identify fine precipitates and analyze concentration profiles of solute elements.

3. Results and Discussion

3.1. The Effects of Single Addition of P on As-cast γ Grain Structure

Figure 1(a) shows the as-cast γ grain structure in the sample with 0.02 mass% P. The bottom and top parts of this figure correspond to the sidewall surface and center of the ingot, respectively. The bright boundary corresponds to the as-cast γ grain boundary. The structure consists of two different grain regions; one is columnar grain region which develops from the mold side to the center and the other is equiaxed grain region which forms at the center part of the ingot. **Figure 1(b)** shows the δ dendrite structure in the same location. The structure consists of columnar dendrite region near the mold side and equiaxed dendrite region at the center. We measured the Secondary Dendrite Arm Spacing (DAS) at various positions along the thickness direction and estimated the cooling rates based on an empirical equa-

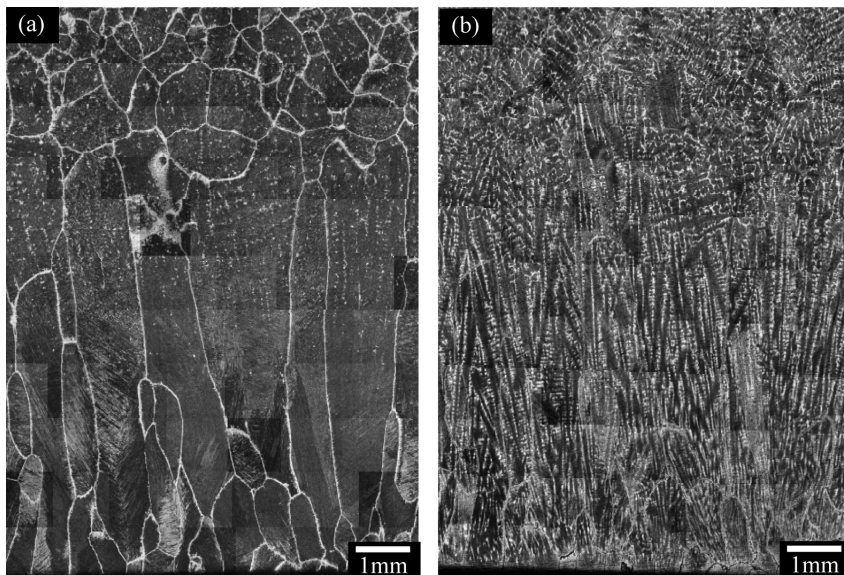


Fig. 1. Microstructures of the sample with 0.04 mass% Al and 0.02 mass% P. (a) As-cast γ grain structure, (b) δ dendrite structure. The two micrographs show the same location in the sample. The top and the bottom of each micrograph correspond to the center of the ingot and the sidewall surface, respectively.

tion, $\lambda_2=710(60T)^{-0.39}$.¹⁷⁾ As is consistent with our previous study, the cooling rates in the present experiments fall within a range of 5–30 K/s which is comparable to that in the conventional continuous casting process of carbon steel slabs.

The addition of P changed the as-cast γ grain structure. In the sample with 0.035 mass% P, very fine grains appear between the columnar and equiaxed grain regions, as can be seen in **Fig. 2**. Then, the as-cast γ grain structure is characterized by three regions; Coarse Columnar Grain (CCG), Fine Columnar Grain (FCG) and Coarse Equiaxed Grain (CEG) regions, while the CEG region was called Equiaxed Grain (EG) region in the previous report.¹⁴⁾ **Figure 3(a)** shows the as-cast γ grain structure in the sample with 0.1 mass% P. The comparison between the structures of

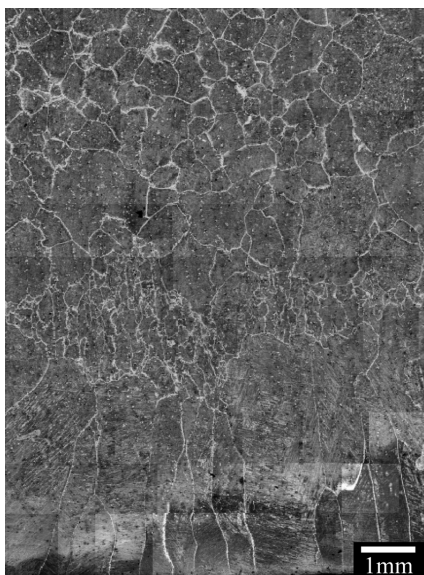


Fig. 2. As-cast γ grain structure of the sample with 0.04 mass% Al and 0.035 mass% P. The top and the bottom of each micrograph correspond to the center of the ingot and the sidewall surface, respectively.

Figs. 1(a) and 3(a) clearly indicates the fact that P addition leads to refinement of as-cast γ grain structure. The structure in Fig. 3(a) consists of very fine columnar and equiaxed grains over the whole observation area, except for the vicinity of the sidewall surface where slightly coarse grains exist. Both the very fine columnar and equiaxed grains were denoted as the FCG in the present study, since it was quite difficult to clearly distinguish between the columnar and equiaxed shapes of the fine grains in some samples. Figure 3(b) shows the δ dendrite structure observed in the same location. The δ dendrite structure consists of the columnar and equiaxed dendrite regions, and it is not substantially different from the δ dendrite structure in the sample with 0.02 mass% P (Fig. 1(b)). By comparing Figs. 3(a) and 3(b), it was observed that each of the fine columnar γ grains forms within one or a few dendrites in the columnar dendrite region, and the short axis diameter of the fine columnar grain is comparable to the size of the primary DAS. Also, each of the fine equiaxed γ grains forms within one columnar or equiaxed dendrite.

As mentioned before, the as-cast γ grain structure consisted of the CCG, FCG and CEG regions. The length of each region along the thickness direction was measured, and it was divided by the length from the sidewall surface to the center of the ingot, *viz.*, 10 mm, in order to obtain a fraction of each region, f_i with $i=\text{CCG}, \text{FCG}$ or CEG . **Figure 4** shows the dependency of the fractions of CCG, FCG and CEG regions on P concentration. The FCG region does not exist when P concentration is less than 0.035 mass%. The increase of P concentration leads to increase of the fraction of FCG region and decrease of the fractions of CCG and CEG regions and, finally, almost fully refined structure without CCG and CEG regions forms with the addition of 0.1 mass% P.

Figure 5 shows the dependency of the as-cast γ grain size in each region on P concentration. The short axis diameter of CCG, $d_{\gamma\text{SCCG}}$, and diameter of CEG, $d_{\gamma\text{CEG}}$, decrease with the increase of P concentration, while the short axis

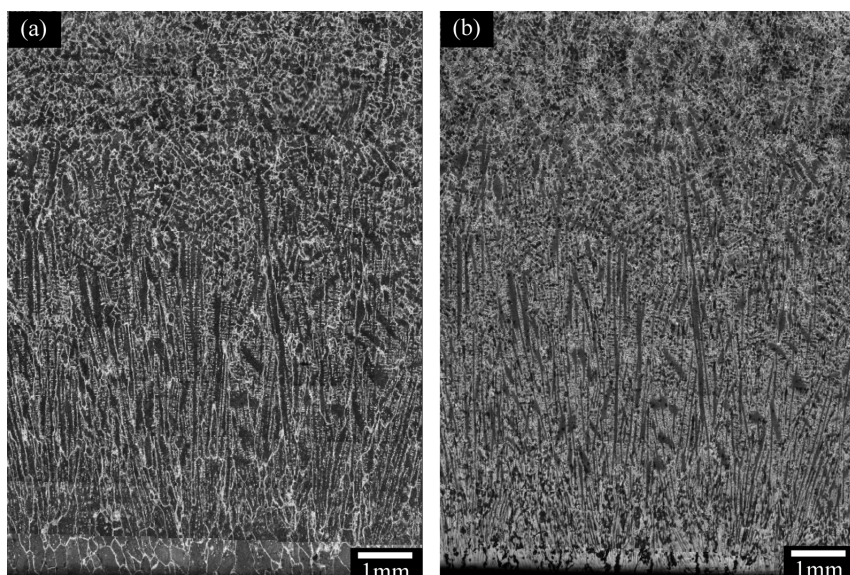


Fig. 3. Microstructures of the sample with 0.04 mass% Al and 0.1 mass% P. (a) As-cast γ grain structure, (b) δ dendrite structure. The two micrographs show the same location in the sample. The top and the bottom of each micrograph correspond to the center of the ingot and the sidewall surface, respectively.

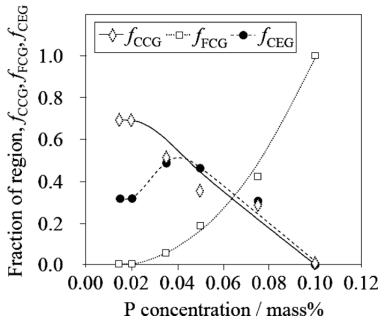


Fig. 4. The effects of P addition on the fractions of CCG, FCG and CEG regions (f_{CCG} , f_{FCG} and f_{CEG}).

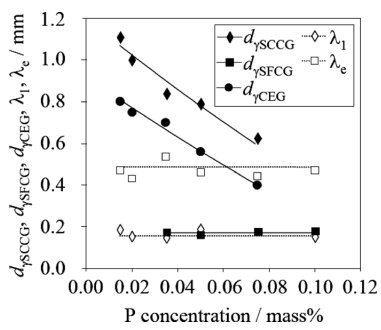


Fig. 5. The effects of P addition on the γ grain sizes. $d_{\gamma\text{SCCG}}$ and $d_{\gamma\text{FCG}}$ represent the short axis diameters of CCG and FCG, respectively. $d_{\gamma\text{CEG}}$ is the diameter of CEG. λ_1 and λ_e are the primary DAS of columnar dendrites and the center-to-center spacing of equiaxed dendrites, respectively.

diameter of FCG, $d_{\gamma\text{FCG}}$, is almost independent of P concentration. In order to demonstrate the correlation between the as-cast γ grain and δ dendrite structures, the primary DAS of columnar dendrites, λ_1 , and the center-to-center spacing of equiaxed dendrites, λ_e , are also presented in Fig. 5. The primary DAS was measured at 4 mm from the sidewall surface where the FCG always existed in the samples with 0.035 to 0.1 mass% P. The primary DAS and center-to-center spacing of equiaxed dendrites are almost constant. Therefore, the size in the δ dendrite structure is not affected by the addition of P. It is important to note that the short axis diameter of FCG is comparable to the primary DAS, which implies that the growth of the FCG was inhibited immediately after the γ transformation/solidification completed.

The phase diagram of Fe–0.2mass%C–0.04mass%Al–0.8mass%Mn–0.2mass%Si–0.006mass%N– x mass%P steel, calculated by CALPHAD method,¹⁸⁾ is given in Fig. 6 where the horizontal axis is P concentration. For this calculation, we employed the thermodynamic database, Pan-Iron.¹⁹⁾ As P concentration increases, both the liquidus and solidus temperatures are lowered, and especially, the solidus temperature is lowered more significantly. Hence it is expected that the stabilized liquid phase might provide pinning effect on the growth of γ grain in the present steel with P addition.

The EPMA analysis was conducted to investigate P concentration profile in the sample. Since the concentration profile in as-cast γ grain structure was focused, the sample used for the EPMA analysis was the one quenched from

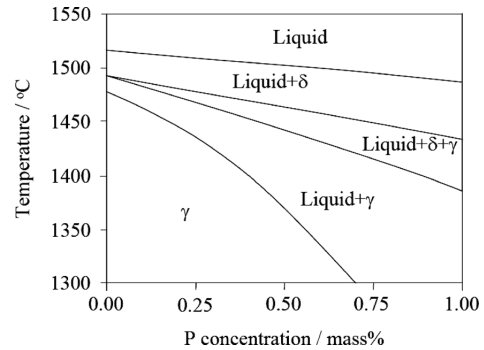


Fig. 6. A phase diagram of Fe–0.2mass%C–0.04mass%Al–0.8mass%Mn–0.2mass%Si–0.006mass%N– x P system obtained from CALPHAD method.

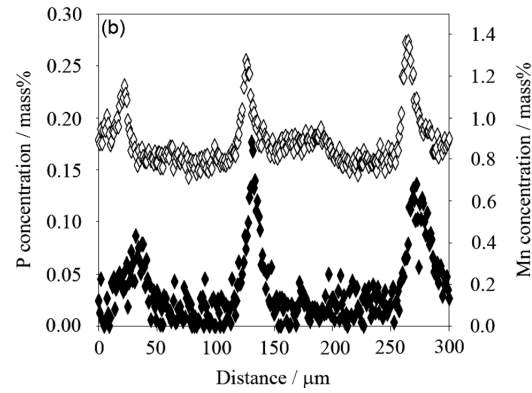
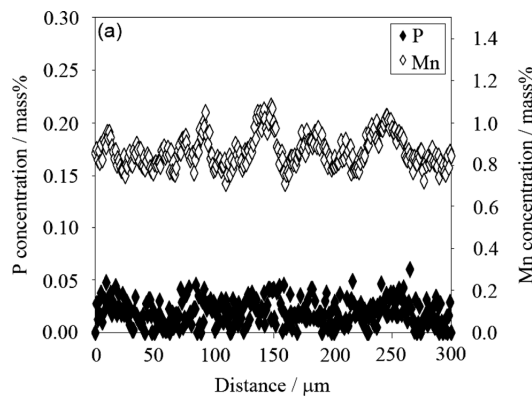


Fig. 7. Concentration profiles of P and Mn in (a) CCG and (b) FCG regions of the cast sample with 0.04 mass% Al and 0.035 mass% P. The scanned direction is parallel to the sidewall surface of the ingot. The full and open symbols are the P and Mn concentrations, respectively.

1 000°C which exhibited the full martensite structure without the pro-eutectoid α -ferrite. The concentration profile was obtained by performing the EPMA analysis for every 1 μm along a 300 μm distance parallel to the sidewall surface in both CCG and FCG regions. Figures 7(a) and 7(b) show the concentration profiles of P (full symbol) in the CCG and FCG regions, respectively, in the sample with 0.035 mass% P. The P concentration in mass% is indicated by the y -axis on the left-hand side, while x -axis represents the distance of EPMA analysis. Segregation of P significantly occurs in the FCG region but not in the CCG region. Furthermore, from detailed comparison between the concentration profile of P and the δ dendrite structure, the enrichment of P was found at interdendritic region, as

expected from the partition coefficient of P, $k_p=0.29$ for δ solidification. As described above, the increase of P concentration lowers T_γ , stabilizing liquid phase at low temperatures. It is considered, therefore, that the refinement of as-cast γ grain structure should originate from the pinning effect of the liquid phase at the interdendritic region stabilized by the P segregation.

The influences of the other elements such as C, Si and Mn are discussed in the following. The diffusion velocity of C in solid and liquid phases is quite high, and therefore, the concentration of C during the solidification process in the present casting condition was considered to become approximately uniform. The EPMA analysis demonstrated that the concentration profiles of Si were almost uniform in both the CCG and FCG regions. This is because the average concentration of Si is relatively low and the partition coefficient of Si is not significantly small, $k_{Si}=0.66$. Hence, the segregations of C and Si were negligible. The concentration profiles of Mn in the CCG and FCG regions are shown in Fig. 7. The Mn concentration in mass% is specified by the open symbol. The segregation of Mn occurs at interdendritic region in the FCG region. From the thermodynamic calculation, however, it was demonstrated that the segregation of Mn does not significantly alter the phase equilibria of this system. Therefore, the segregation of Mn may lead to only small effect on the as-cast grain structure and the refinement should be mainly ascribable to the segregation of P.

The mechanism of the refinement of the as-cast γ grain structure by the segregation of P is explained as follows. As indicated in Figs. 7(a) and 7(b), the microsegregation of P in FCG region is significant, compared with that in CCG region. It has been demonstrated in several studies²⁰⁻²⁴⁾ that in directionally solidified or mold cast samples, the degree of microsegregation increases as the distance from the mold wall increases, which is consistent with our observation. Several mechanisms were proposed to explain this phenomenon, *e.g.*, increase in partial solidification time,²³⁾ increase in dendrite tip undercooling,²⁵⁾ decrease in partition coefficient^{20,22,25)} and change in morphology of δ dendrite structure.¹⁴⁾ Furthermore, the convection flow in the liquid due to pouring, thermal convection or density difference should promote mass transfer from the solid/liquid solidification front toward the center of ingot, which lead to increase in the average concentration in the liquid and accordingly increment of the degree of microsegregation. Although it remains to clarify which mechanism is dominant, the degree of microsegregation of P increases from the mold side to the center of ingot in the present casting experiment. After the formation of columnar δ dendrite, the CCG forms in the vicinity of the mold wall and the CCG develops into the center of ingot along the thickness direction. In the sample without P addition, the growth of the CCG will continues until the equiaxed γ grains form from the equiaxed δ dendrite and these grains retard the development of the CCG. In the sample with P addition, the P segregation at interdendritic region of columnar dendrite gradually increases as the distance from the mold wall increases, which results in the stabilization of liquid phase at lower temperatures. Then, the development of CCG was stopped by the existence of the stabilized liquid phase, *viz.*, the pinning

effect of liquid phase. Ahead of the CCG, a fine grain structure develops on the columnar/equiaxed dendrite in an elongated shape in the thickness direction of ingot, while the grain growth along the direction perpendicular to the thickness direction is inhibited by existence of the stabilized liquid phase. As the result, the FCG forms subsequently to the CCG formation. In the center of the ingot, the cooling rate becomes low, which reduces the P segregation and, hence, the γ grains can coarsen, resulting in the formation of the CEG in the sample with low P concentration. In the sample with high P concentration, the P segregation substantially occurs in the center part of the ingot and, hence, the f_{CEG} decreases with the increase in P concentration in Fig. 4. This point will be discussed in more detail later in the next section. It is noted that the value of f_{CEG} firstly increases from 0.02 to 0.035 mass% P in Fig. 4. In the sample with 0.035 mass% P, the effect of P segregation is not very substantial and it leads to decrement of CCG region and the formation of the small FCG region. In this case, as mentioned above, the P segregation at the center should be reduced due to the low cooling rate. Hence, these conditions lead to the slight increment of f_{CEG} . On the other hand, in the sample with P concentration higher than 0.075 mass%, the fraction of CEG region decreases because the P segregation at the center becomes significant despite the low cooling rate. Figure 5 shows that the short axis diameter of CCG and diameter of CEG decrease with the increase of P concentration. Importantly, the size of CEG is eventually reduced to the size of FCG. It is seen in Fig. 6 that the T_γ was reduced by P addition, even though the P segregation does not occur substantially. Hence the refinement regarding the short axis diameter of the CCG should be attributed to the lowering of T_γ over the whole sample by the P addition. In the following section, we will discuss the effects of simultaneous additions of Al and P.

3.2. Effects of Simultaneous Additions of Al and P on As-cast γ Grain Structure

The as-cast γ grain structure in the samples with simultaneous additions of Al and P similarly consisted of the CCG, FCG and CEG regions. Figure 8 shows the dependency of the fraction of FCG region on Al concentration in the samples with different P concentrations. It can be seen that the fraction of FCG region increases with the increase of Al concentrations. It is important to note that less amount of P concentration is required to obtain the refinement of the as-cast γ grain structure when Al is added. Moreover, the complete refinement, *viz.*, fully fine γ grain structure

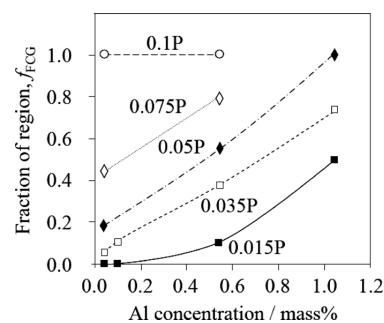


Fig. 8. The dependency of fraction of FCG region, f_{FCG} , on Al and P concentrations.

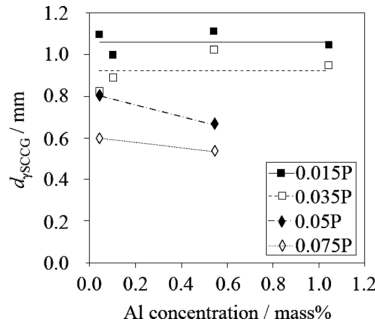


Fig. 9. The dependency of short axis diameter of CCG, $d_{y\text{SCCG}}$, on Al and P concentrations.

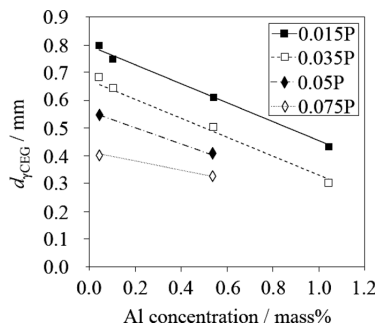


Fig. 10. The dependency of diameter of CEG, $d_{y\text{CEG}}$, on Al and P concentrations.

was observed in the samples with 0.05 mass% P and 1.04 mass% Al.

As discussed in the Sec. 3.1, the short axis diameter of CCG and the diameter of CEG are reduced by the P addition. The effects of simultaneous additions of Al and P on the as-cast γ grain sizes in CCG, CEG and FCG regions are discussed below. From the microstructural analysis, it was found that the short axis diameters of FCG are almost independent of Al concentration. However, the short axis diameter of CCG very slightly decreases while the diameter of CEG obviously decreases with the increase of Al concentration, as shown in Figs. 9 and 10, respectively. The mechanism for the refinement by Al addition is explained in the followings.

As was consistent with our previous study on the effects of Al addition,¹⁴⁾ the present EPMA analysis showed that the AlN particles did not exist in the samples with 0.04 and 0.1 mass% Al, and they were rarely dispersed in the samples with 0.54 and 1.04 mass% Al. Consequently, the AlN should not be responsible for the refinement described in Fig. 8. In the previous study, it was discussed that the Al addition reduces the partition coefficient of P during solidification process and hence, it enhances the P segregation, which results in the pinning effect of high temperature phase, liquid or δ phase depending on the Al concentration, on the as-cast γ grain structure. However, the direct evidence for this mechanism was not yet provided in the previous study. Figure 11(a) represents the result of the EPMA analysis for the FCG region in the sample with 0.54mass%Al–0.035mass%P–0.2mass%C. The concentration profiles of Al and P are specified by the open and full symbols, respectively. The concentration profile of Al is almost flat with slight peaks observed at dendrite stems. On the other hand, the P segregation is clearly observed. Figure

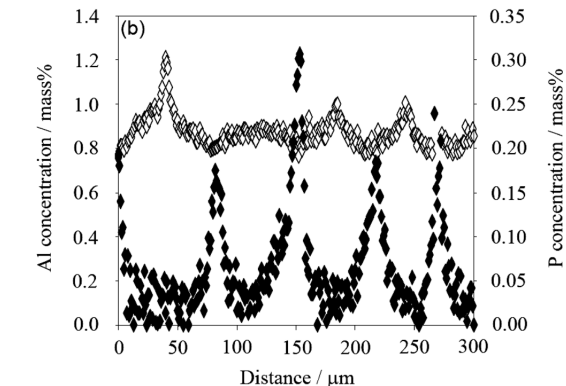
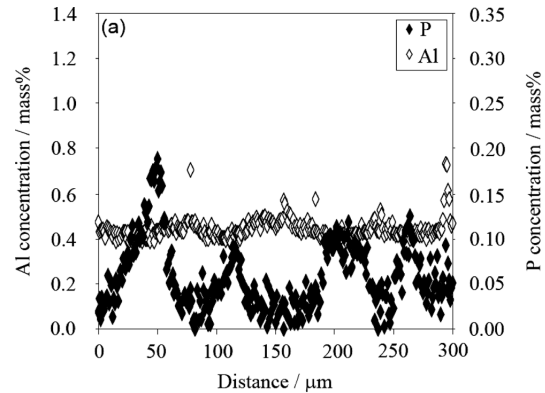


Fig. 11. Concentration profiles of Al and P in the FCG region of the cast samples with (a) 0.54 mass% Al and (b) 1.04 mass% Al. The P concentrations in the two samples are 0.035 mass%. The scanned direction is parallel to the sidewall surface of the ingot. The full and open symbols are the P and Al concentrations, respectively.

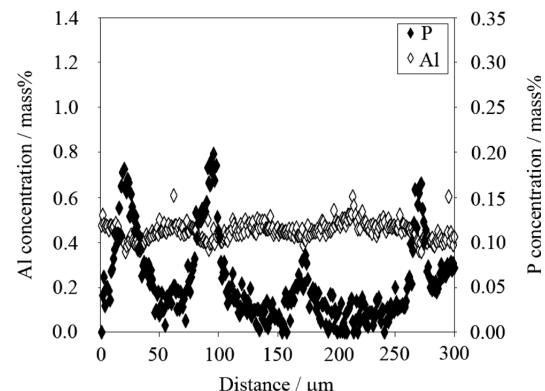


Fig. 12. Concentration profiles of Al and P in the CEG region of the cast samples with 0.54 mass% Al and 0.035 mass% P. The scanned direction is parallel to the sidewall surface of the ingot. The full and open symbols are the P and Al concentrations, respectively.

11(b) demonstrates the concentrations profiles of Al and P in the FCG region in the sample with 1.04mass%Al–0.035mass%P–0.2mass%C. The concentration profile of Al is approximately considered to be flat. Importantly, the comparison between Figs. 11(a) and 11(b) clearly indicates the fact that the Al addition enhances the segregation of P. Furthermore, Figure 12 shows the result of the EPMA analysis for the CEG region in the sample with 0.54mass%Al–0.035mass%P–0.2mass%C. The degree of P segregation in the CEG region is quite comparable to that in

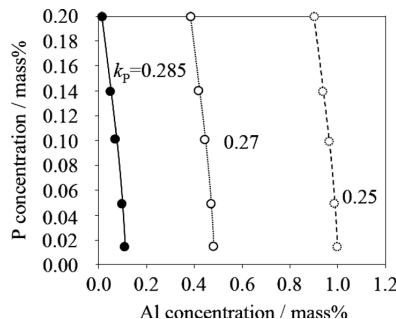


Fig. 13. The dependency of partition coefficient of P at liquidus temperature, k_p , on Al concentration in the samples with different P concentrations obtained from CALPHAD method.

the FCG region represented in Fig. 11(a). It is hence expected the P segregation in the CEG region may lead to the pinning effect.

In the present study, it was demonstrated that the simultaneous additions of Al and P lead to the refinement of the as-cast γ grain structure, which originates from the P segregation enhanced by the Al addition. Figure 12 shows the contour lines of partition coefficient of P at the liquidus temperature in the P and Al concentrations plane obtained by the CALPHAD method. The partition coefficient of P fairly decreases with increase of Al concentration in the range of our focus. The decrease of the partition coefficient by the Al addition hence contributes to the enhancement of P segregation, as observed in Fig. 11.

4. Conclusions

In the present study, the effects of single addition of P and simultaneous additions of Al and P on the as-cast γ grain structure in 0.2 mass% C steel were investigated by means of the permanent mold casting experiments. The following points obtained in this study are important to be summarized:

(1) The as-cast γ grain structure consists of Coarse Columnar Grain (CCG), Fine Columnar Grain (FCG) and Coarse Equiaxed Grain (CEG) regions in the present casting condition. The addition of P increases the FCG region and reduces the CCG and CEG regions.

(2) The short axis diameter of the CCG and the diameter of CEG decrease with the increase of P concentration. However, the short axis diameter of the FCG is almost independent of P concentration and it is comparable to the primary DAS of columnar dendrite.

(3) The refinement by the P addition is ascribable to the segregation of P developed at the interdendritic region, which significantly lowers the temperature for completion of γ transformation/solidification, T_{γ} .

(4) The simultaneous additions of Al and P result in the refinement of the as-cast γ grain structure. Importantly, the complete refinement of the γ grain structure, viz., a fine grain structure without the CCG and CEG regions was observed with small amount of P when Al was added.

(5) The refinement by simultaneous additions of Al and P is ascribable to the P segregation enhanced by the Al addition.

REFERENCES

- 1) O. Tsubakihara: *Trans. Iron Steel Inst. Jpn.*, **27** (1987), 81.
- 2) N. Zapuskalov: *ISIJ Int.*, **43** (2003), 1115.
- 3) L. Schmidt and A. Josefsson: *Scand. J. Metall.*, **3** (1974), 193.
- 4) N. Yoshida, Y. Kobayashi and K. Nagai: *Tetsu-to-Hagané*, **90** (2004), 198.
- 5) L. T. Shiang and P. J. Wray: *Metall. Trans. A*, **20A** (1989), 1191.
- 6) Y. Maehara, K. Yasumoto, Y. Sugitani and K. Gunji: *Trans. Iron Steel Inst. Jpn.*, **25** (1985), 1045.
- 7) N. S. Pottore, C. I. Garcia and A. J. DeArdo: *Metall. Trans. A*, **22A** (1991), 1871.
- 8) O. Umezawa, N. Yoshida, K. Hirata, T. Higuchi, N. Sakuma and K. Nagai: *J. Adv. Sci.*, **13** (2001), 175.
- 9) K. Hirata, O. Umezawa and K. Nagai: *Mater. Trans.*, **43** (2002), 305.
- 10) N. Yoshida, O. Umezawa and K. Nagai: *ISIJ Int.*, **43** (2003), 348.
- 11) M. Ohno and K. Matsuura: *ISIJ Int.*, **48** (2008), 1373.
- 12) M. Sasaki, K. Matsuura, K. Ohsasa and M. Ohno: *Tetsu-to-Hagané*, **94** (2008), 31.
- 13) S. Tsuchiya, M. Ohno, K. Matsuura and K. Isobe: *Tetsu-to-Hagané*, **95** (2009), 1.
- 14) S. Kencana, M. Ohno, K. Matsuura and K. Isobe: *ISIJ Int.*, **50** (2010), 231.
- 15) T. Maruyama, K. Matsuura, M. Kudoh and Y. Itoh: *Tetsu-to-Hagané*, **85** (1999), 585.
- 16) T. Maruyama, M. Kudoh and Y. Itoh: *Tetsu-to-Hagané*, **86** (2000), 14.
- 17) A. Suzuki, T. Suzuki, Y. Nagaoka and Y. Iwata: *J. Jpn. Inst. Met.*, **32** (1968), 1301.
- 18) L. Kaufman and H. Bernstein: Computer Calculation of Phase Diagrams with Special Reference to Refractory Materials, Academic Press, New York, (1970), 1.
- 19) <http://www.computherm.com/databases.html>.
- 20) R. D. Doherty and D. A. Melford: *J. Iron Steel Inst.*, **204** (1966), 1131.
- 21) T. Z. Kattamis and M. C. Flemings: *Trans. AIME*, **223** (1965), 992.
- 22) F. Weinberg and E. Teghtsoonian: *Metall. Trans.*, **3** (1972), 93.
- 23) D. A. Granger and T. F. Bower: *J. Inst. Met.*, **98** (1970), 353.
- 24) P. J. Ahearn and C. Quigley: *J. Iron Steel Inst.*, **204** (1966), 16.
- 25) M. Sugiyama, T. Umeda and J. Matsuyama: *Tetsu-to-Hagané*, **60** (1974), 1094.